Evidence against Broad Dibaryons

R. L. Shypit[(a)] and D. V. Bugg
Queen Mary College, London E1 4NS, United Kingdom

D. M. Lee, M. W. McNaughton, and R. R. Silbar
Los Alamos National Laboratory, Los Alamos, New Mexico 87545

N. M. Stewart
Royal Holloway and Bedford New College, London T20 0EX, United Kingdom

A. S. Clough
University of Surrey, Guildford, Surrey, United Kingdom

C. L. Hollas,[(b)] K. H. McNaughton, and P. Riley
University of Texas, Austin, Texas 78712

and

C. A. Davis
University of Manitoba, Winnipeg, Manitoba, Canada R3T 2N2
(Received 28 October 1987)

Spin-correlation parameters A_{LL}, A_{SL}, A_{NL}, A_{N0}, A_{S0}, A_{L0}, and A_{0L} have been measured for the reaction $pp \rightarrow np\pi^+$ at 492, 576, 643, 729, and 796 MeV. An isobar analysis determines magnitudes and phases of partial waves up to $NN\ {}^3F_3$. For the amplitude $NN({}^1D_2) \rightarrow N\Delta({}^5S_2)$, the phase shows a strong threshold enhancement in the $N\Delta$ channel, dropping from $44.4° \pm 4.4°$ at 492 MeV to $11.9° \pm 1.9°$ at 796 MeV. Other phases show little activity. Broad dibaryons are conclusively ruled out in ${}^1D_2$, ${}^3F_3$, and ${}^3P_2$ in this energy range.

PACS numbers: 13.75.Cs, 14.20.Pt

There has been considerable speculation on the existence of dibaryon resonances[1] in the mass range 2110 to 2250 MeV/c^2, accessible in pp scattering with beams of 500 to 800 MeV. A recent review has been given by Locher, Sainio, and Svarc.[2] Most of the evidence comes from the NN elastic channel and $NN \rightarrow \pi d$. However, branching ratios to NN and πd are small ($< 15\%$), and the remaining channel width can lie only in $NN\pi$, dominantly $N\Delta$. Unambiguous identification of a resonance would therefore be a large and rapid phase increase with laboratory energy in a partial wave for $NN \rightarrow N\Delta$. Prime candidates are $NN\ {}^1D_2$, ${}^3F_3$, and ${}^3P_2$.

We report measurements on $pp \rightarrow np\pi^+$ made at the Clinton P. Anderson Meson Physics Facility with a longitudinally polarized target and a beam whose polarization was oriented successively normal (N) to the $n\Delta$ production plane, sideways (S), and longitudinally (L). Observables A_{SL}, A_{NL}, A_{N0}, A_{S0}, A_{L0}, and A_{0L} depend on interferences and hence are phase sensitive. The parameter A_{LL} depends on amplitudes squared, but with opposite signs for triplet and singlet initial states; it is crucial in separation of ${}^1D_2$ from ${}^3F_3$ and ${}^3P_1$ amplitudes. From these observables, we determine low partial waves in both magnitude and phase.

Two previous experiments along these lines have been reported. Waltham *et al.*[3] measured A_{N0}, A_{0N}, A_{SS}, A_{NN}, and A_{LL} at 420, 465, and 510 MeV at TRIUMF. Present results have statistics a factor 10 better near 500 MeV. Wicklund *et al.*[4] measured A_{N0}, A_{S0}, and A_{L0} with high statistics at the Argonne zero-gradient synchrotron at 569, 806, 1012, and 1253 MeV. Our measurements extend significantly the number of observables and are more closely spaced in energy.

First we describe the experiment briefly; details will be given in a later publication. The polarized propanediol target was 2 cm in diameter and 4 cm long. The field was provided by superconducting Helmholtz coils, leaving conical apertures upstream and downstream with 48° half angle, and an aperture of ±10.5° around 90°. All three final-state particles were detected in coincidence. The proton and π^+ were tracked in pairs of multiwire proportional chambers and drift chambers covering as much as possible of all three apertures in the magnet. Nucleons emerged within the downstream aperture. Pions were also detected near 90° and in the backward cone (down to 70 MeV/c); wide coverage of the geometry was important in the determination of amplitudes uniquely and accurately.

Neutrons were converted with 25% efficiency in a position-sensitive scintillator array[5] 105 cm square×30 cm thick, 4.5 m from the target; time of flight was measured with ± 0.75-ns accuracy with respect to both accelerator rf and scintillators triggering on charged particles. The positional accuracy was ± 3.5 cm horizontally and ± 7.5 cm vertically. The range of neutron angles was covered with $13°$, $25°$, and $37.5°$ settings of this detector.

With the momenta of the p and π^+ treated as unknowns, events were subjected to a two-constraint fit. The quality of signal observed is illustrated in Fig. 1(a); the background subtraction was checked with a dummy target at 492 and 796 MeV.

The beam spot was 2-3-mm diam, and centering on the target was monitored precisely by a pair of trigger counters which detected pp elastic events around $90°$ c.m. The beam intensity, $\simeq 1.25\times 10^6$/s, was measured to $\pm 1\%$ with an ionization chamber. Beam polarization was monitored to $\pm 1\%$ absolute accuracy by the quench technique[6] and also with an upstream four-arm polarimeter. Target polarization was measured by standard NMR techniques with an absolute accuracy of $\pm 4\%$ and relative errors of $\pm 1\%$; it was checked with $\pm 4\%$ absolute accuracy with pp elastic scattering.

We now turn to analysis. It is convenient to think in terms of the process $pp \rightarrow nX^{++}$, where $X = \Delta$ or $X = S$, the πN S wave. Other small πN partial waves are neglected. The calculations include amplitudes for $pp \rightarrow pX^+$ with appropriate Clebsch-Gordan coefficients; here both the πN S_{31} and S_{11} waves are included, in the latter case with the assumption that the exchanged meson has isospin 1. The kinematic variables in which data are binned are as follows: M, the mass of X^{++}; β, the polar angle of the neutron in the overall c.m. system; θ and ϕ, the polar and azimuthal angles of the π^+ from X^{++} decay with respect to the neutron direction in the X^{++} rest frame. For every event, N and S components of beam polarization are resolved onto the production plane of nX^{++}.

Asymmetries are determined in $3\times 5\times 5\times 4$ bins of M, β, θ, and ϕ, respectively. At 492 (796) MeV, there are 163 (296) bins significantly populated. Statistics are 101×10^3 events at 492 MeV after background subtraction, rising to 381×10^3 at 796 MeV. In Fig. 1, one-dimensional projections display some of the gross features of the data, together with fits from the isobar analysis. There are important multidimensional correlations, fitted in the analysis; in particular, A_{NL}, A_{S0}, A_{L0}, and A_{0L} appear only as functions of $\sin\theta\cos\theta\sin\phi$, $\sin^2\theta\sin 2\phi$, and $\sin\theta\sin\phi$, as shown in Eq. (21) of Ref. 4. All the data show only small energy dependence, immediately suggesting that resonances are absent.

Each partial wave is expressed in the form

$$F(M,\beta,\theta,\phi,s) = a(s) f(M) g(\beta,\theta,\phi) \times \exp\{i[\delta_{NN}(s) + \delta_{NX}(s)]\}.$$

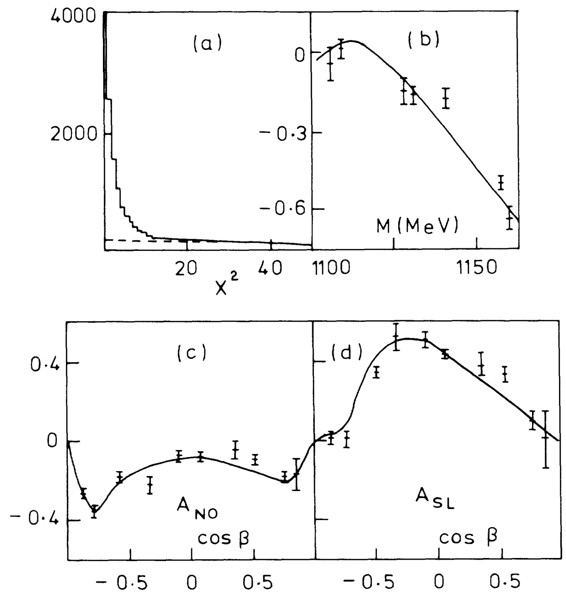

FIG. 1. (a) χ^2 distribution of events at 796 MeV, with the dummy data shown dashed; (b) projection of A_{LL} onto M at 492 MeV; (c),(d) projection of A_{N0} and A_{SL} onto $\cos\beta$ at 729 MeV. Solid lines in (b)-(d) are fits from the amplitude analysis.

Here, $f(M)$ fits πN phase shifts; for the Δ it has a Breit-Wigner dependence on M. The standard angular-momentum decomposition is expressed by $g(\beta,\theta,\phi)$. Initial- and final-state interactions are expressed via δ_{NN}, the phase shift in NN elastic scattering, and δ_{NX}, a parameter which becomes the NX elastic phase shift in the limit of weak scattering; $a(s)$ is real.

High partial waves are taken from the π-exchange predictions of Kloet and Silbar[7] (KS), namely for $^3F_4$ and above in the NN channel, or for orbital angular momentum $L_{N\Delta} \geq 2$ in the $N\Delta$ channel. In order to retain quantitative contact with π exchange, the strengths of low partial waves for $NN \rightarrow N\Delta$ will be expressed in the form of a scaling factor N times the KS prediction. For $^3P_1 \rightarrow {}^3P_1$ and $^3P_1 \rightarrow {}^5P_1$, N and $\delta_{N\Delta}$ are the same within errors, and final fits assume common values; the same is true for $^3P_2$.

Amplitudes for $NN \rightarrow NS$ are included only for initial $^3P_1$ and $^1D_2$ states; other partial waves are zero within errors and phases δ_{NS} are everywhere compatible with zero within errors. The $NN \rightarrow NS$ $^3P_1 \rightarrow {}^3S_1$ amplitude is essential in fitting of data below the Δ peak. Figure 1(b) shows a projection onto M; the dramatic rise in A_{LL} at low M is due to this amplitude, which alone would give $A_{LL} = +1$, while the other large amplitude at this energy, $NN \rightarrow N\Delta$ $^1D_2 \rightarrow {}^5S_2$, gives $A_{LL} = -1$.

The outcome of the analysis is given in Table I. Extensive tests have demonstrated that further freedom in the fits is not demanded by these data; explicitly, freeing

TABLE I. Fitted phases $\delta_{N\Delta}$ and scaling factors N for $NN \rightarrow N\Delta$ amplitudes. Amplitudes a for $NN \rightarrow NS$ are on an absolute, energy-independent, scale. Values in parentheses have been fixed. Phases are in degrees.

		Energy (MeV) 492	576	643	729	796
$\delta_{N\Delta}$	$^1S_0 \rightarrow {}^5D_0$	(0.0)	(−4.0)	−7.8 ± 3.5	−12.8 ± 3.5	−12.8 ± 2.8
	$^3P_0 \rightarrow {}^3P_0$	(0.0)	(0.0)	−0.8 ± 3.4	5.3 ± 2.8	−3.3 ± 3.0
	$^3P_1 \rightarrow {}^3P_1, {}^5P_1$	(0.0)	(4.2)	(9.8)	14.7 ± 2.9	15.1 ± 2.5
	$^3P_2, {}^3F_2 \rightarrow {}^3P_2, {}^5P_2$	−21.8 ± 3.25	−26.3 ± 2.9	−27.3 ± 4.7	−36.8 ± 2.1	−29.3 ± 2.1
	$^1D_2 \rightarrow {}^5S_2$	44.4 ± 4.4	37.4 ± 3.1	31.1 ± 2.2	20.3 ± 2.0	11.9 ± 1.9
	$^3F_3 \rightarrow {}^5P_3$	(2.0)	(4.0)	5.9 ± 2.4	6.0 ± 2.1	4.8 ± 1.9
N	$^1S_0 \rightarrow {}^5D_0$	(7.4)	(7.4)	(7.4)	7.25 ± 0.53	7.39 ± 0.44
	$^3P_0 \rightarrow {}^3P_0$	8.39 ± 0.87	8.39 ± 0.80	8.54 ± 0.43	7.41 ± 0.26	6.16 ± 0.23
	$^3P_1 \rightarrow {}^3P_1, {}^5P_1$	2.01 ± 0.33	1.45 ± 0.22	1.11 ± 0.05	1.09 ± 0.04	1.24 ± 0.04
	$^3P_2 \rightarrow {}^3P_2, {}^5P_2$	7.26 ± 0.48	7.36 ± 0.45	5.61 ± 0.22	3.87 ± 0.16	3.44 ± 0.14
	$^1D_2 \rightarrow {}^5S_2$	(0.851)	(0.771)	(0.751)	(0.741)	(0.739)
	$^1D_2 \rightarrow {}^3D_2, {}^5D_2$	(1.0)	(1.0)	(1.0)	(1.17)	1.34 ± 0.07
	$^3F_2 \rightarrow {}^3P_2, {}^5P_2$	(1.0)	(1.0)	(1.0)	(0.93)	0.89 ± 0.04
	$^3F_3 \rightarrow {}^5P_3$	1.03 ± 0.25	1.53 ± 0.11	1.44 ± 0.09	1.26 ± 0.03	1.15 ± 0.03
a	$^3P_1 \rightarrow {}^3S_1$	1.75 ± 0.19	1.68 ± 0.11	1.10 ± 0.07	0.60 ± 0.06	0.34 ± 0.05
	$^1D_2 \rightarrow {}^3P_2$	0.14 ± 0.04	0.10 ± 0.04	(0.0)	(0.0)	(0.0)
	χ^2	1159	1060	2140	2634	3898
	Data points	1141	1141	1946	2072	2072

any single partial wave beyond those of Table I reduces χ^2 by < 20, even at 796 MeV. Such extra freedom has very little effect on the dominant partial waves $^1D_2$, $^3F_3$, and $^3P_2$ $NN \rightarrow N\Delta$, which are the prime dibaryon candidates, but the determination of the smaller amplitudes deteriorates. The errors of Table I allow for statistics and uncertainties in parametrization of πN S waves, but do not allow for systematic errors in high partial waves nor the omission of πN P_{11}, P_{31}, and P_{13} waves.

The magnitude of the dominant $^1D_2$ amplitude is chosen to fit the accurately known inelasticity in NN elastic phase-shift analysis, after allowance for $NN \rightarrow \pi d$. Absolute phases are well determined at 643 MeV and above by interference with high partial waves (largely $^1G_4$), which provide a reference phase. At 492 and 576 MeV, the reference phase is provided roughly equally by high partial waves and by the $NN \rightarrow NS$ $^3P_1 \rightarrow {}^3S_1$ amplitude; the latter is particularly valuable and was not fitted quantitatively by Wicklund *et al.*

Magnitudes of amplitudes follow the trends of NN elastic phase-shift analysis,[8] but should be much more precise. There, it is well known that the KS amplitudes are a little high for $^1D_2$, slightly low for $^3F_3$, and a factor 3 to 7 too low for $^3P_2$. For $^1S_0$ and $^3P_0$, the KS predictions are exceedingly small, so that the large scaling factors of Table I still give modest amplitudes. The magnitude of the $^1S_0$ amplitude is the most poorly determined feature of the whole fit, and at low energies has to be constrained to a value taken from high energies.

The intriguing feature of the results is the structure of the S-wave $N\Delta$ phase (Fig. 2). Waltham *et al.*[3] and Wicklund *et al.*[4] reported a similar result, though their determination of absolute phases was considerably less precise. This threshold attraction is reminiscent of the NN elastic $^1S_0$ and $^3S_1$ states, and relates naturally to them in a quark model. A strong effect has also been observed in $\Lambda N \rightarrow \Lambda N$ at the ΣN threshold.[9] An account of the energy dependence of Fig. 2 down to threshold will require a coupled-channels analysis of the opening of the $N\Delta$ channel, coupled to NN and πd. The TRIUMF data of Waltham *et al.*[3] from 420 to 510 MeV, when analyzed with our program, confirm that the S-wave $\delta_{N\Delta}$ peaks at $\simeq 45°$, with no variation within errors from 420 to 510 MeV; it is fixed accurately by interference with the other dominant amplitude $NN \rightarrow NS$ $^3P_1 \rightarrow {}^3S_1$ in A_{N0}, A_{0N}, and A_{SL}. Thus the threshold attraction is not strong enough to create a resonance or bound state, though there must be some nearby singularity.

We have considered the possibility that the S-wave

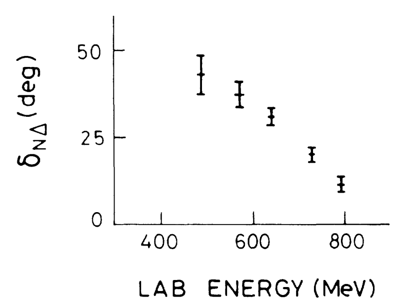

FIG. 2. The phase $\delta_{N\Delta}$ for $^1D_2 \rightarrow {}^5S_2$.

$N\Delta$ phase is a disguised form of the *np* final-state interaction. Extensive tests including this final-state interaction explicitly eliminate this possibility. We observe a threshold spike in the number of events against NN mass. However, phase-sensitive observables, notably A_{N0} and A_{SL}, show no effect at low NN mass. The conclusion is that the NN final-state interaction projects roughly equally into all $N\Delta$ and NS partial waves, and therefore has little effect on spin observables, as predicted by Dubach, Kloet, and Silbar.[10] At most, it could account for 20% of the S-wave $\delta_{N\Delta}$.

Values of $\delta_{N\Delta}$ for $^3P_2$ and $^3F_3$ are negative or small and show no signs of resonance. The $^3P_2$ phase is well determined at all energies. The $^3F_3$ phase is very stable at the higher energies, but tends to drift positive at the lowest two energies, with a small improvement in χ^2. Since we expect this phase to increase from threshold as $\bar{k}^3$, where $\bar{k}$ is the mean c.m. momentum in the final state, we constrain it (and those of $^1S_0$, $^3P_0$, and $^3P_1$) at the lowest two energies. We suggest that all these phases are characteristic of the opening of an inelastic threshold.

Summarizing, our conclusions are that (1) the absence of a rapid phase increase rules out broad $^1D_2$, $^3P_2$, and $^3F_3$ dibaryons in this mass range, and (2) there is an attractive threshold $N\Delta$ interaction in the $^1D_2 \rightarrow {}^5S_2$ channel. It will be interesting to see the effect of this S-wave attraction on Δ-nucleus physics and the equation of state of nuclear matter at high densities, and whether or not there is sufficient attraction to lead to a pion condensate.

We acknowledge gratefully the assistance of the Clinton P. Anderson Meson Physics Facility operating crews and the polarized-target group, led by Dr. J. Jarmer. We thank Dr. J. Simmons for the loan of the polarized-target cryostat and the multiwire proportional chamber electronics. This work was supported by the U.S. Department of Energy and by the United Kingdom Science and Engineering Research Council.

[a]Present address: Jet Propulsion Laboratory, Pasadena, CA 91109.

[b]Present address: Los Alamos National Laboratory, Los Alamos, NM 87545.

[1]K. Hidaka *et al.*, Phys. Lett. **70B**, 479 (1977).

[2]M. P. Locher, M. E. Sainio, and A. Svarc, Adv. Nucl. Phys. **17**, 47 (1986).

[3]C. E. Waltham *et al.*, Nucl. Phys. **A433**, 649 (1985).

[4]A. B. Wicklund *et al.*, Phys. Rev. D **35**, 2670 (1987).

[5]A. S. Clough *et al.*, Phys. Rev. C **21**, 988 (1980).

[6]G. G. Ohlsen *et al.*, Phys. Rev. Lett. **27**, 599 (1971); M. W. McNaughton *et al.*, Phys. Rev. C. **23**, 1128 (1981); M. W. McNaughton and E. P. Chamberlin, Phys. Rev. C **24**, 1778 (1981).

[7]W. M. Kloet and R. R. Silbar, Nucl. Phys. **A338**, 281 (1980).

[8]R. A. Arndt, J. S. Hyslop, III, and L. D. Roper, Phys. Rev. D **35**, 128 (1987).

[9]C. Pigot *et al.*, Nucl. Phys. **B249**, 172 (1985).

[10]J. Dubach, W. M. Kloet, and R. R. Silbar, Phys. Rev. C **33**, 373 (1986).